

RSIR Transformer: Hierarchical Vision Transformer using Random Sampling Windows and Important Region Windows

Zhemin Zhang¹, Xun Gong¹

¹Southwest Jiaotong University
zheminzhang@my.swjtu.edu.cn

Abstract

Recently, Transformers have shown promising performance in various vision tasks. However, the high costs of global self-attention remain challenging for Transformers, especially for high-resolution vision tasks. Local self-attention runs attention computation within a limited region for the sake of efficiency, resulting in insufficient context modeling as their receptive fields are small. In this work, we introduce two new attention modules to enhance the global modeling capability of the hierarchical vision transformer, namely, random sampling windows (RS-Win) and important region windows (IR-Win). Specifically, RS-Win sample random image patches to compose the window, following a uniform distribution, i.e., the patches in RS-Win can come from any position in the image. IR-Win composes the window according to the weights of the image patches in the attention map. Notably, RS-Win is able to capture global information throughout the entire model, even in earlier, high-resolution stages. IR-Win enables the self-attention module to focus on important regions of the image and capture more informative features. Incorporated with these designs, RSIR-Win Transformer demonstrates competitive performance on common vision tasks.

1 Introduction

Modeling in computer vision has long been dominated by convolutional neural networks (CNNs). Recently, transformer models in the field of natural language processing (NLP) [Devlin *et al.*, 2018; Vaswani *et al.*, 2017; Yates *et al.*, 2021] have attracted great interest from computer vision (CV) researchers. The Vision Transformer (ViT) [Dosovitskiy *et al.*, 2020] model and its variants have gained state-of-the-art results on many core vision tasks [Zhao *et al.*, 2020; Touvron *et al.*, 2021]. The original ViT, inherited from NLP, first splits an input image into patches, while equipped with a trainable class (CLS) token that is appended to the input patch tokens. Then, patches are treated in the same way as tokens in NLP applications, using self-attention layers for global information communication, and finally using the output CLS

token for prediction. Recent work [Dosovitskiy *et al.*, 2020; Liu *et al.*, 2021] shows that ViT outperforms state-of-the-art convolutional networks [Huang *et al.*, 2018] on large-scale datasets. However, when trained on smaller datasets, ViT usually underperforms its counterparts based on convolutional layers.

The original ViT lacks inductive bias, such as locality and translation equivariance, which leads to overfitting and data inefficient usage. To improve data efficiency, numerous efforts have studied how to introduce the locality of the CNN model into the ViT to improve its scalability [Chu *et al.*, 2021a; Yang *et al.*, 2021]. These methods typically reintroduce hierarchical architectures to compensate for the loss of non-locality, such as the Swin Transformer [Liu *et al.*, 2021].

Local self-attention and hierarchical ViT (LSAH-ViT) has been demonstrated to solve data inefficiency and alleviate model overfitting. However, LSAH-ViT uses window-based attention at shallow layers, losing the non-locality of original ViT, which leads to LSAH-ViT having limited model capacity and henceforth scales unfavorably on larger datasets such as ImageNet-21K [Dai *et al.*, 2021]. To bridge the connection between windows, previous LSAH-ViT works propose specialized designs such as the “haloing operation” [Vaswani *et al.*, 2021] and “shifted window” [Liu *et al.*, 2021]. These approaches often need complex architectures, and their receptive field is increased quite slowly and requires stacking many blocks to achieve global self-attention.

In this paper, we propose two novel types of Transformer modules, called random sampling windows (RS-Win) and important region windows (IR-Win). RS-Win sample random image patches to compose the window, following a uniform distribution, i.e., the patches in RS-Win can come from any position in the image, shown in Figure 1(e). RS-Win can perform both local and global spatial interactions in a single block. Compared to the previously handcrafted sparse attention, RS-Win gives greater flexibility. The number of patches randomly sampled in each window of RS-Win is fixed, and computing self-attention locally within windows, thus the complexity becomes linear to image size.

To make the model have not only “randomness” but also “determinism”, we use IR-Win to make the model focus on important regions of the feature map. IR-Win first uses a method similar to that in CBAM [Woo *et al.*, 2018] to infer the at-



Figure 1: Full attention and its sparse variants. (a) Full attention is a global operation that is computationally expensive and requires a lot of memory. (b) Swin Transformer uses partitioned window attention. (c) Cross-shaped attention parallel computes the self-attention of horizontal and vertical stripes that form a cross-shaped window. (d) Grid attention attends globally to patches in a sparse, uniform grid overlaid on the entire 2D space. (e) Random sampling attention sample random patches compose a window and perform self-attention within the window. (f) Important region attention composes the window according to the weights of the image patches in the attention map. The same colors are spatially mixed by the self-attention operation.

attention map of the input feature map, which marks which regions of the image are important for the recognition task. With the attention map determined, the next step is to sample according to the attention map. That is, patches with high attention weights compose a window, and similarly, patches with low weights compose other windows, as shown in Figure 1(f). Here, we can simply view RS-Win as "exploration", whose purpose is to freely "explore" which image patches are important in the image. The purpose of IR-Win is to integrate important image patches obtained from "exploration" into the same window for information interaction. By combining RS-Win and IR-Win, each local window can flexibly explore the entire image space and receive data-dependent local information, facilitating learning more complex relations.

Based on the proposed RS-Win and IR-Win self-attention, we design a general vision transformer backbone with a hierarchical architecture, named RSIR Transformer. Our tiny variant RSIR-T achieves 83.9% Top-1 accuracy on ImageNet-1K without any extra training data.

2 Related Work

Transformers were proposed by Vaswani et al. [Vaswani et al., 2017] for machine translation, and have since become the state-of-the-art method in many NLP tasks. Recently, ViT [Dosovitskiy et al., 2020] demonstrates that pure Transformer-based architectures can also achieve very competitive results. One challenge for vision transformer-based models is data efficiency. Although ViT [Dosovitskiy et al., 2020] can perform better than convolutional networks with hundreds of millions of images for pre-training, such a data requirement is difficult to meet in many cases.

To improve data efficiency, many recent works have focused on introducing the locality and hierarchical structure of convolutional neural networks into ViT, proposing a series of local and hierarchical ViT. The Swin Transformer [Liu et al., 2021] pays attention on shifted windows in a hierarchical architecture. Nested ViT [Zhang et al., 2022] proposes a block aggregation module, which can more easily achieve cross-block non-local information communication. Focal ViT [Yang et al., 2021] presents focal self-attention, each token attends its closest surrounding tokens at fine granularity and the

Algorithm 1: Pseudocode of RS-Win in a PyTorch-like style.

```

Input: x.shape=B, L, C (batch, length, dim)
# sample_map from uniform distribution
sample_map = torch.rand(B, L, device=x.device)
# Sort sample_map for each token sequence
ids_shuffle = torch.argsort(sample_map, dim=1)
# ids_restore for sequence restore
ids_restore = torch.argsort(ids_shuffle, dim=1)
# Shuffle token sequence by ids_shuffle
x_shuffle = torch.gather(x, dim=1,
    index=ids_shuffle.unsqueeze(-1).repeat(1, 1, C))
# Partition windows
x_windows = window_partition(x_shuffle,
    window_size)
# Windows self-attention
attn_windows = self.attn(x_windows)
# Reverse windows
x = window_reverse(attn_windows, window_size, H,
    W)
# Restore the token sequence
x_restore = torch.gather(x, dim=1,
    index=ids_restore.unsqueeze(-1).repeat(1, 1, C))

```

tokens far away at coarse granularity, which can effectively capture both short- and long-range visual dependencies.

Based on the local window, a series of local self-attentions with different shapes are proposed in subsequent work. Axial self-attention [Ho *et al.*, 2019] and criss-cross attention [Huang *et al.*, 2019] achieve longer-range dependencies in horizontal and vertical directions respectively by performing self-attention in each single row or column of the feature map. CSWin [Dong *et al.*, 2022] proposed a cross-shaped window self-attention region, including multiple rows and columns. MaxViT [Tu *et al.*, 2022] proposed grid attention, the grid attention module attends globally to pixels in a sparse, uniform grid overlaid on the entire 2D space. The performance of the above attention mechanisms are either limited by the restricted window size or has a high computation cost, which cannot achieve a better trade-off between computation cost and global-local interaction.

This paper proposes a new hierarchical vision Transformer backbone by introducing RS-Win and IR-Win self-attention. MaxViT [Tu *et al.*, 2022] is the most related works with our RSIR Transformer. Compared to it, RSIR Transformer not only gives greater flexibility for global information communication, but also has data-dependent local information communication.

3 Method

3.1 Random Sampling Windows Self-Attention

LSAH-ViT uses window-based attention at shallow layers, lacking the non-locality of original ViT, which leads to LSAH-ViT having limited model capacity and henceforth scales unfavorably on larger datasets. Existing works use specialized designs, such as the “haloing operation” [Vaswani *et*

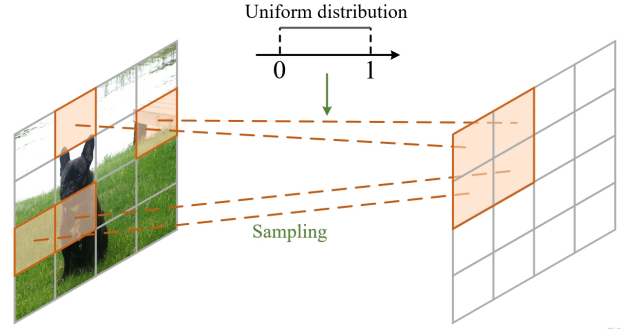


Figure 2: RS-Win self-attention

al., 2021] and “shifted window” [Liu *et al.*, 2021], to communicate information between windows. These approaches often need complex architectures, and their receptive field is increased quite slowly and requires stacking many blocks to achieve global self-attention. For capturing dependencies varied from short-range to long-range, we propose RS-Win self-attention. Compared to the previously handcrafted sparse attention, RS-Win gives greater flexibility.

RS-Win sample random image patches to compose the window, following a uniform distribution, i.e., the patches in RS-Win can come from any position in the image, shown in Figure 2. The RS-Win algorithm is summarized with Pytorch-like pseudo code in Algorithm 1.

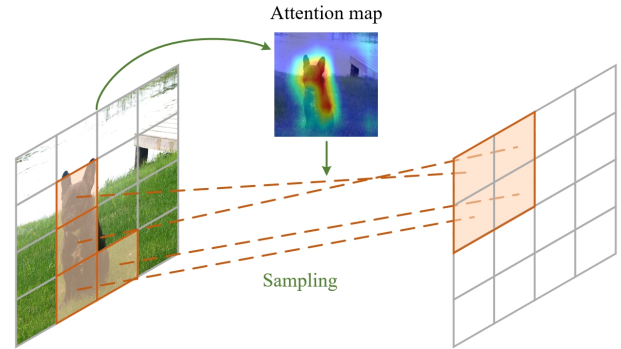


Figure 3: IR-Win self-attention

3.2 Important Region Windows Self-Attention

To make the model have not only “randomness” but also “determinism”, we use IR-Win to make the model focus on important regions of the feature map. IR-Win first uses a method similar to that in CBAM [Woo *et al.*, 2018] to infer the attention map of the input feature map, which marks which regions of the image are important for the recognition task. With the attention map determined, the next step is to sample according to the attention map. That is, patches with high attention weights compose a window, and similarly, patches with low weights compose other windows, as shown in Figure 3. IR-Win enables local information communication to become data-dependent, thereby facilitating the model’s ability to distinguish redundant information. The IR-Win algorithm is summarized with Pytorch-like pseudo code in Algorithm 2.

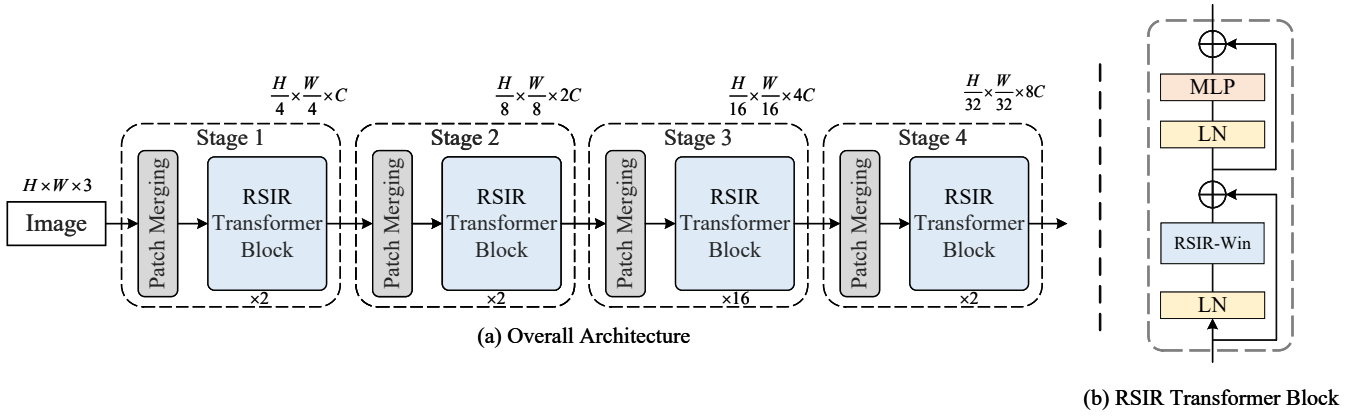


Figure 4: Left: The overall architecture of our RSIR Transformer, Right: The composition of each block.

Algorithm 2: Pseudocode of IR-Win in a PyTorch-like style.

```

Input: x.shape=B, L, C (batch, length, dim)
# sample_map from attention map
with torch.no_grad():
    sample_map = torch.mean(x,dim=2)
# Sort sample_map for each token sequence
ids_shuffle = torch.argsort(sample_map, dim=1)
# ids_restore for sequence restore
ids_restore = torch.argsort(ids_shuffle, dim=1)
# Shuffle token sequence by ids_shuffle
x_shuffle = torch.gather(x, dim=1,
    index=ids_shuffle.unsqueeze(-1).repeat(1, 1, C))
# Partition windows
x_windows = window_partition(x_shuffle,
    window_size)
# Windows self-attention
attn_windows = self.attn(x_windows)
# Reverse windows
x = window_reverse(attn_windows, window_size, H,
    W)
# Restore the token sequence
x_restore = torch.gather(x, dim=1,
    index=ids_restore.unsqueeze(-1).repeat(1, 1, C))

```

3.3 Parallel Implementation

We split the K heads into two parallel groups, $K/2$ heads per group, thus incorporating two different attention mechanisms, as shown in Figure 5. The first group of heads perform RS-Win attention, the second group of heads perform IR-Win attention. Finally, the outputs of these two parallel groups will be concatenated back together.

$$\text{head}_k = \begin{cases} \text{RS-MSA}_k(X) & k = 1, \dots, K/2 \\ \text{IR-MSA}_k(X) & k = K/2 + 1, \dots, K \end{cases} \quad (1)$$

$$\text{RSIR-Win}(X) = \text{Concat}(\text{head}_1, \dots, \text{head}_K) W^O \quad (2)$$

where $W^O \in R^{C \times C}$ is the commonly used projection matrix that is used to integrate the output tokens of two groups.

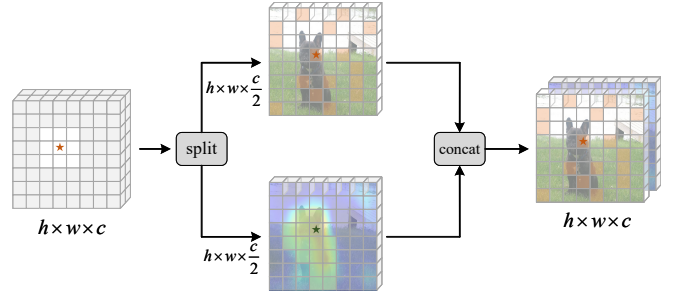


Figure 5: A parallel implementation of RSIR-Win.

Compared to the step-by-step implementation of RS-Win and IR-Win self-attention separately, such a parallel mechanism allows the incorporation of RS-Win and IR-Win information in each block and has a lower computation complexity.

3.4 RSIR Transformer Block

Equipped with the above self-attention mechanism, RSIR Transformer block is formally defined as:

$$\begin{aligned} \hat{X}^l &= \text{RSIR-Win}(\text{LN}(X^{l-1})) + X^{l-1}, \\ X^l &= \text{MLP}(\text{LN}(\hat{X}^l)) + \hat{X}^l \end{aligned} \quad (3)$$

where \hat{X}^l and X^l denote the output features of the RSIR-Win module and the MLP module for block l , respectively.

3.5 Overall Architecture

An overview architecture of the RSIR-ViT is presented in Figure 4 (a), which illustrates the tiny version. RSIR-ViT consists of four hierarchical stages, like Swin-ViT [Liu *et al.*, 2021] to build hierarchical architecture to capture multi-scale features. Each stage contains a patch merging layer and several RSIR Transformer blocks. As the network gets deeper, the input features are spatially downsampled by a certain ratio through the patch merging layer. The channel dimension is expanded twice to produce a hierarchical image representation. Specifically, the spatial downsampling ratio is set to

Table 1: Object detection and instance segmentation performance on the COCO val2017 with the Mask R-CNN framework and 1x training schedule. The models have been pre-trained on ImageNet-1K. The resolution used to calculate FLOPs is 800×1280.

Backbone	Params	FLOPs	AP ^{box}	AP ₅₀ ^{box}	AP ₇₅ ^{box}	AP ^{mask}	AP ₅₀ ^{mask}	AP ₇₅ ^{mask}
ResNet-50 [He <i>et al.</i> , 2016]	44M	260G	38.0	58.6	41.4	34.4	55.1	36.7
Twins-S [Chu <i>et al.</i> , 2021a]	44M	228G	42.7	65.6	46.7	39.6	62.5	42.6
PVT-S [Wang <i>et al.</i> , 2021]	44M	245G	40.4	62.9	43.8	37.8	60.1	40.3
Swin-T [Liu <i>et al.</i> , 2021]	48M	264G	43.7	66.6	47.6	39.8	63.3	42.7
CSWin-T [Dong <i>et al.</i> , 2022]	42M	279G	46.7	68.6	51.3	42.2	65.6	45.4
MaxViT-T [Tu <i>et al.</i> , 2022]	49M	286G	46.9	69.1	52.0	42.2	66.1	46.3
RSIR-T (ours)	42M	279G	47.6	69.2	52.3	42.7	66.3	46.6
RegNeXt-101-64 [He <i>et al.</i> , 2016]	101M	493G	42.8	63.8	47.3	38.4	60.6	41.3
Twins-L [Chu <i>et al.</i> , 2021a]	120M	474G	45.2	67.5	49.4	41.2	64.5	44.5
PVT-L [Wang <i>et al.</i> , 2021]	81M	364G	42.9	65.0	46.6	39.5	61.9	42.5
Swin-B [Liu <i>et al.</i> , 2021]	107M	496G	46.9	–	–	42.3	–	–
CSWin-B [Dong <i>et al.</i> , 2022]	97M	526G	48.7	70.4	53.9	43.9	67.8	47.3
MaxViT-B [Tu <i>et al.</i> , 2022]	103M	589G	48.9	70.5	54.1	43.8	67.9	47.6
RSIR-B (ours)	96M	517G	49.2	71.0	54.1	44.5	68.1	47.7

4 in the first stage and 2 in the last three stages. The outputs of the patch merging layer are fed into the subsequent RSIR Transformer block, and the number of tokens is kept constant. Finally, we apply a global average pooling step on the output of the last block to obtain the image representation vector for the final prediction.

Table 2: Detailed configurations of RSIR Transformer Variants.

Models	#Dim	#Blocks	#heads	#Param.
RSIR-T	64	2,2,16,2	4,4,8,16	22M
RSIR-B	96	2,4,24,2	4,8,16,32	85M

Variants. For a fair comparison with other vision Transformers under similar settings, we designed two variants of the proposed RSIR Transformer: RSIR-T (Tiny) and RSIR-B (Base). Table 2 shows the detailed configurations of all variants. They are designed by changing the block number of each stage and the base channel dimension C . The RSIR-T’s head numbers for the four stages are 4, 4, 8, 16; the RSIR-B’s head numbers are 4, 8, 16, 32.

4 Experiments

To show the effectiveness of the RSIR Transformer, we conduct experiments on ImageNet-1K [Deng *et al.*, 2009]. We then compare the performance of RSIR and state-of-the-art Transformer backbones on small datasets Caltech-256 [Griffin *et al.*, 2007] and Mini-ImageNet [Krizhevsky *et al.*, 2012]. To further demonstrate the effectiveness and generalization of our backbone, we conduct experiments on ADE20K [Zhou *et al.*, 2017] for semantic segmentation, and COCO [Lin *et al.*, 2014] for object detection. Finally, we perform comprehensive ablation studies to analyze each component of the RSIR Transformer.

4.1 Classification on the ImageNet-1K

Implementation details. This setting mostly follows [Liu *et al.*, 2021]. We use the PyTorch toolbox [Paszke *et al.*, 2019]

Table 3: Comparison of different models on ImageNet-1K.

Method	Image Size	Param.	FLOPs	Top-1 acc.
RegNetY-4G [Radosavovic <i>et al.</i> , 2020]	224 ²	21M	4.0G	80.0
DeiT-S [Touvron <i>et al.</i> , 2021]	224 ²	22M	4.6G	79.8
PVT-S [Wang <i>et al.</i> , 2021]	224 ²	25M	3.8G	79.8
Swin-T [Liu <i>et al.</i> , 2021]	224 ²	29M	4.5G	81.3
CSWin-T [Dong <i>et al.</i> , 2022]	224 ²	23M	4.3G	82.7
MaxViT-T [Tu <i>et al.</i> , 2022]	224 ²	29M	5.6G	83.6
RSIR-T (ours)	224 ²	22M	5.0G	83.9
RegNetY-16G [Radosavovic <i>et al.</i> , 2020]	224 ²	84M	16.0G	82.9
ViT-B [Dosovitskiy <i>et al.</i> , 2020]	384 ²	86M	55.4G	77.9
DeiT-B [Touvron <i>et al.</i> , 2021]	224 ²	86M	17.5G	81.8
PVT-B [Wang <i>et al.</i> , 2021]	224 ²	61M	9.8G	81.7
Swin-B [Liu <i>et al.</i> , 2021]	224 ²	88M	15.4G	83.3
CSWin-B [Dong <i>et al.</i> , 2022]	224 ²	78M	15.0G	84.2
MaxViT-B [Tu <i>et al.</i> , 2022]	224 ²	120M	23.4G	84.9
RSIR-B (ours)	224 ²	85M	16.3G	85.1

to implement all our experiments. We employ an AdamW [Kingma and Ba, 2014] optimizer for 300 epochs using a cosine decay learning rate scheduler and 20 epochs of linear warm-up. A batch size of 256, an initial learning rate of 0.001, and a weight decay of 0.05 are used. ViT-B/16 uses an image size 384×384 and others use 224×224. We include most of the augmentation and regularization strategies of Swin transformer [Liu *et al.*, 2021] in training.

Results. Table 3 compares the performance of the proposed RSIR Transformer with the state-of-the-art CNN and Vision Transformer backbones on ImageNet-1K. Compared to ViT-B, the proposed RSIR-B model is +7.2% better and has much lower computation complexity than ViT-B. Meanwhile, the proposed RSIR Transformer variants outperform the state-of-the-art Transformer-based backbones, and is +0.3% higher than the most related MaxViT Transformer. RSIR Transformer has the low computation complexity compared to all models in Table 3. For example, RSIR-T achieves 83.9% Top-1 accuracy with only 5.0G FLOPs. And for the base model setting, our RSIR-B also achieves the best performance.

Table 4: Comparison of different models on Caltech-256.

Method	Image Size	Param.	FLOPs	Top-1 acc.
Swin-T [Liu <i>et al.</i> , 2021]	224 ²	29M	4.5G	43.3
CSWin-T [Dong <i>et al.</i> , 2022]	224 ²	23M	4.3G	47.7
MaxViT-T [Tu <i>et al.</i> , 2022]	224 ²	29M	5.6G	47.9
RSIR-T (ours)	224 ²	22M	5.0G	48.8
ViT-B [Dosovitskiy <i>et al.</i> , 2020]	384 ²	86M	55.4G	37.6
Swin-B [Liu <i>et al.</i> , 2021]	224 ²	88M	15.4G	46.7
CSWin-B [Dong <i>et al.</i> , 2022]	224 ²	78M	15.0G	48.5
MaxViT-B [Tu <i>et al.</i> , 2022]	224 ²	120M	23.4G	48.6
RSIR-B (ours)	224 ²	85M	16.3G	49.2

4.2 Classification on Caltech-256 and Mini-ImageNet

Implementation details. Follow most of the experimental settings in the above subsection and change epochs to 100.

Results. In Table 4 and Table 5, we compare the proposed RSIR Transformer with state-of-the-art Transformer architectures on small datasets. With the limitation of pages, we only compare with a few classical methods here. It is known that ViTs usually perform poorly on such tasks as they typically require large datasets to be trained on. The models that perform well on large-scale ImageNet do not necessarily work perform on small-scale Mini-ImageNet and Caltech-256, e.g., ViT-B has top-1 accuracy of 58.3% and Swin-B has top-1 accuracy of 67.4% on the Mini-ImageNet, which suggests that ViTs are more challenging to train with less data. The proposed RSIR can significantly improve the data efficiency and performs well on small datasets such as Caltech-256 and Mini-ImageNet. Compared with MaxViT, it has increased by 0.9% and 0.3% respectively.

Table 5: Comparison of different models on Mini-ImageNet.

Method	Image Size	Param.	FLOPs	Top-1 acc.
Swin-T [Liu <i>et al.</i> , 2021]	224 ²	29M	4.5G	66.3
CSWin-T [Dong <i>et al.</i> , 2022]	224 ²	23M	4.3G	66.8
MaxViT-T [Tu <i>et al.</i> , 2022]	224 ²	29M	5.6G	67.9
RSIR-T (ours)	224 ²	22M	5.0G	68.4
ViT-B [Dosovitskiy <i>et al.</i> , 2020]	384 ²	86M	55.4G	58.3
Swin-B [Liu <i>et al.</i> , 2021]	224 ²	88M	15.4G	67.4
CSWin-B [Dong <i>et al.</i> , 2022]	224 ²	78M	15.0G	68.4
MaxViT-B [Tu <i>et al.</i> , 2022]	224 ²	120M	23.4G	68.6
RSIR-B (ours)	224 ²	85M	16.3G	69.1

4.3 COCO Object Detection

Implementation details. We use the Mask R-CNN [He *et al.*, 2017] framework to evaluate the performance of the proposed RSIR Transformer backbone on the COCO benchmark for object detection. We pretrain the backbones on the ImageNet-1K dataset and apply the finetuning strategy used in Swin Transformer [Liu *et al.*, 2021] on the COCO training set.

Results. We compare RSIR Transformer with various backbones, as shown in Table 1. It shows that the proposed RSIR Transformer variants clearly outperform all the CNN and Transformer counterparts. For object detection, our RSIR-T and RSIR-B achieve 47.6 and 49.2 box mAP for object detection, surpassing the previous best CSWin Transformer by +0.7 and +0.3, respectively. We also achieve similar performance gain on instance segmentation.

Table 6: Comparison of the segmentation performance of different backbones on the ADE20K. All backbones are pretrained on ImageNet-1K with the size of 224 × 224. The resolution used to calculate FLOPs is 512 × 2048.

Backbone	Params	FLOPs	SS mIoU	MS mIoU
Twins-S [Chu <i>et al.</i> , 2021a]	55M	905G	46.2	47.1
Swin-T [Liu <i>et al.</i> , 2021]	60M	945G	44.5	45.8
CSWin-T [Dong <i>et al.</i> , 2022]	60M	959G	49.3	50.4
MaxViT-T [Tu <i>et al.</i> , 2022]	71M	989G	49.5	50.7
RSIR-T (ours)	57M	956G	49.9	51.2
Twins-L [Chu <i>et al.</i> , 2021a]	113M	1164G	48.8	50.2
Swin-B [Liu <i>et al.</i> , 2021]	121M	1188G	48.1	49.7
CSWin-B [Dong <i>et al.</i> , 2022]	109M	1222G	50.8	51.7
MaxViT-B [Tu <i>et al.</i> , 2022]	125M	1221G	51.3	52.6
RSIR-B (ours)	109M	1210G	51.9	52.7

4.4 ADE20K Semantic Segmentation

Implementation details. We further investigate the capability of RSIR Transformer for Semantic Segmentation on the ADE20K [Zhou *et al.*, 2017] dataset. Here we employ the widely-used UperNet [Xiao *et al.*, 2018] as the basic framework and followed Swin’s [Liu *et al.*, 2021] experimental settings. In Table 6, we report both the single-scale (SS) and multi-scale (MS) mIoU for better comparison.

Results. As shown in Table 6, our RSIR variants outperform previous state-of-the-arts under different configurations. Specifically, our RSIR-T and RSIR-B outperform the MaxViT by +0.4% and +0.6% SS mIoU, respectively. These results show that the proposed RSIR Transformer can effectively capture the context dependencies of different distances.

4.5 Ablation Study

We perform ablation studies on image classification and downstream tasks for the fundamental designs of our RSIR Transformer. For a fair comparison, we use the Swin-T [Liu *et al.*, 2021] as the backbone for the following experiments, and only change one component for each ablation.

Attention Mechanism Comparison. In this subsection, we compare with existing self-attention mechanisms. As shown in Table 7, the proposed RSIR self-attention mechanism performs better than the existing self-attention mechanism.

Table 7: Comparison of different self-attention mechanisms.

	ImageNet top-1	COCO AP ^{box}	ADE20k SS mIoU
Swin’s shifted windows [Liu <i>et al.</i> , 2021]	81.3	43.7	44.5
Spatially Sep [Chu <i>et al.</i> , 2021a]	81.5	44.2	45.8
Sequential Axial [Ho <i>et al.</i> , 2019]	81.5	41.5	42.9
Criss-Cross [Huang <i>et al.</i> , 2019]	81.7	44.5	45.9
Cross-shaped [Dong <i>et al.</i> , 2022]	82.2	45.0	46.2
Grid [Tu <i>et al.</i> , 2022]	82.5	45.2	46.2
RSIR (ours)	82.9	45.5	46.3

5 Conclusions

In this paper, we have presented a new Vision Transformer architecture named RSIR-Win Transformer. The core design of RSIR-Win Transformer consists of two components: random sampling windows (RS-Win) and important region windows

(IR-Win). RS-Win can sample patches anywhere in the image, increasing the flexibility of the model’s global information flow. IR-Win uses an attention map of input features for sampling, and the composed window is data-dependent. On the other hand, the RSIR-Win Transformer performs RS-Win and IR-Win self-attention in parallel by splitting the multi-heads into two parallel groups. This multi-head grouping design allows the model to efficiently incorporate information from both components without extra computation cost. RSIR-Win Transformer can achieve state-of-the-art performance on ImageNet-1K image classification, COCO object detection and ADE20K semantic segmentation.

References

- [Chu *et al.*, 2021a] Xiangxiang Chu, Zhi Tian, Yuqing Wang, Bo Zhang, Haibing Ren, Xiaolin Wei, Huaxia Xia, and Chunhua Shen. Twins: Revisiting the design of spatial attention in vision transformers. In M. Ranzato, A. Beygelzimer, Y. Dauphin, P.S. Liang, and J. Wortman Vaughan, editors, *Advances in Neural Information Processing Systems*, volume 34, pages 9355–9366. Curran Associates, Inc., 2021.
- [Chu *et al.*, 2021b] Xiangxiang Chu, Bo Zhang, Zhi Tian, Xiaolin Wei, and Huaxia Xia. Do we really need explicit position encodings for vision transformers? *CoRR*, abs/2102.10882, 2021.
- [Dai *et al.*, 2021] Zihang Dai, Hanxiao Liu, Quoc V Le, and Mingxing Tan. Coatnet: Marrying convolution and attention for all data sizes. In M. Ranzato, A. Beygelzimer, Y. Dauphin, P.S. Liang, and J. Wortman Vaughan, editors, *Advances in Neural Information Processing Systems*, volume 34, pages 3965–3977. Curran Associates, Inc., 2021.
- [Deng *et al.*, 2009] Jia Deng, Wei Dong, Richard Socher, Li-Jia Li, Kai Li, and Li Fei-Fei. Imagenet: A large-scale hierarchical image database. In *2009 IEEE Conference on Computer Vision and Pattern Recognition*, pages 248–255, 2009.
- [Devlin *et al.*, 2018] Jacob Devlin, Ming-Wei Chang, Kenton Lee, and Kristina Toutanova. BERT: pre-training of deep bidirectional transformers for language understanding. *CoRR*, abs/1810.04805, 2018.
- [Dong *et al.*, 2022] Xiaoyi Dong, Jianmin Bao, Dongdong Chen, Weiming Zhang, Nenghai Yu, Lu Yuan, Dong Chen, and Baining Guo. Cswin transformer: A general vision transformer backbone with cross-shaped windows. In *Proceedings of the IEEE/CVF Conference on Computer Vision and Pattern Recognition (CVPR)*, pages 12124–12134, June 2022.
- [Dosovitskiy *et al.*, 2020] Alexey Dosovitskiy, Lucas Beyer, Alexander Kolesnikov, Dirk Weissenborn, Xiaohua Zhai, Thomas Unterthiner, Mostafa Dehghani, Matthias Minderer, Georg Heigold, Sylvain Gelly, Jakob Uszkoreit, and Neil Houlsby. An image is worth 16x16 words: Transformers for image recognition at scale. *CoRR*, abs/2010.11929, 2020.
- [Griffin *et al.*, 2007] Gregory Griffin, Alex Holub, and Pietro Perona. Caltech-256 object category dataset. 2007.
- [He *et al.*, 2016] Kaiming He, Xiangyu Zhang, Shaoqing Ren, and Jian Sun. Deep residual learning for image recognition. In *Proceedings of the IEEE Conference on Computer Vision and Pattern Recognition (CVPR)*, June 2016.
- [He *et al.*, 2017] Kaiming He, Georgia Gkioxari, Piotr Dollár, and Ross Girshick. Mask r-cnn. In *Proceedings of the IEEE International Conference on Computer Vision (ICCV)*, Oct 2017.
- [Ho *et al.*, 2019] Jonathan Ho, Nal Kalchbrenner, Dirk Weissenborn, and Tim Salimans. Axial attention in multidimensional transformers. *CoRR*, abs/1912.12180, 2019.
- [Huang *et al.*, 2018] Gao Huang, Shichen Liu, Laurens van der Maaten, and Kilian Q. Weinberger. Condensenet: An efficient densenet using learned group convolutions. In *Proceedings of the IEEE Conference on Computer Vision and Pattern Recognition (CVPR)*, June 2018.
- [Huang *et al.*, 2019] Zilong Huang, Xinggang Wang, Lichao Huang, Chang Huang, Yunchao Wei, and Wenyu Liu. Ccnet: Criss-cross attention for semantic segmentation. In *Proceedings of the IEEE/CVF International Conference on Computer Vision (ICCV)*, October 2019.
- [Kingma and Ba, 2014] Diederik P Kingma and Jimmy Ba. Adam: A method for stochastic optimization. *arXiv preprint arXiv:1412.6980*, 2014.
- [Krizhevsky *et al.*, 2012] Alex Krizhevsky, Ilya Sutskever, and Geoffrey E Hinton. Imagenet classification with deep convolutional neural networks. *Advances in neural information processing systems*, 25:1097–1105, 2012.
- [Lin *et al.*, 2014] Tsung-Yi Lin, Michael Maire, Serge Belongie, James Hays, Pietro Perona, Deva Ramanan, Piotr Dollár, and C. Lawrence Zitnick. Microsoft coco: Common objects in context. In David Fleet, Tomas Pajdla, Bernt Schiele, and Tinne Tuytelaars, editors, *Computer Vision – ECCV 2014*, pages 740–755, Cham, 2014. Springer International Publishing.
- [Liu *et al.*, 2021] Ze Liu, Yutong Lin, Yue Cao, Han Hu, Yixuan Wei, Zheng Zhang, Stephen Lin, and Baining Guo. Swin transformer: Hierarchical vision transformer using shifted windows. In *Proceedings of the IEEE/CVF International Conference on Computer Vision (ICCV)*, pages 10012–10022, October 2021.
- [Paszke *et al.*, 2019] Adam Paszke, Sam Gross, Francisco Massa, Adam Lerer, James Bradbury, Gregory Chanan, Trevor Killeen, Zeming Lin, Natalia Gimelshein, Luca Antiga, et al. Pytorch: An imperative style, high-performance deep learning library. *Advances in neural information processing systems*, 32:8026–8037, 2019.
- [Radosavovic *et al.*, 2020] Ilija Radosavovic, Raj Prateek Kosaraju, Ross Girshick, Kaiming He, and Piotr Dollár. Designing network design spaces. In *Proceedings of the IEEE/CVF Conference on Computer Vision and Pattern Recognition (CVPR)*, June 2020.

- [Touvron *et al.*, 2021] Hugo Touvron, Matthieu Cord, Matthijs Douze, Francisco Massa, Alexandre Sablayrolles, and Herve Jegou. Training data-efficient image transformers-amp; distillation through attention. In Marina Meila and Tong Zhang, editors, *Proceedings of the 38th International Conference on Machine Learning*, volume 139 of *Proceedings of Machine Learning Research*, pages 10347–10357. PMLR, 18–24 Jul 2021.
- [Tu *et al.*, 2022] Zhengzhong Tu, Hossein Talebi, Han Zhang, Feng Yang, Peyman Milanfar, Alan Bovik, and Yinxiao Li. Maxvit: Multi-axis vision transformer. In Shai Avidan, Gabriel Brostow, Moustapha Cissé, Giovanni Maria Farinella, and Tal Hassner, editors, *Computer Vision – ECCV 2022*, pages 459–479, Cham, 2022. Springer Nature Switzerland.
- [Vaswani *et al.*, 2017] Ashish Vaswani, Noam Shazeer, Niki Parmar, Jakob Uszkoreit, Llion Jones, Aidan N Gomez, Łukasz Kaiser, and Illia Polosukhin. Attention is all you need. In I. Guyon, U. Von Luxburg, S. Bengio, H. Wallach, R. Fergus, S. Vishwanathan, and R. Garnett, editors, *Advances in Neural Information Processing Systems*, volume 30. Curran Associates, Inc., 2017.
- [Vaswani *et al.*, 2021] Ashish Vaswani, Prajit Ramachandran, Aravind Srinivas, Niki Parmar, Blake Hechtman, and Jonathon Shlens. Scaling local self-attention for parameter efficient visual backbones. In *Proceedings of the IEEE/CVF Conference on Computer Vision and Pattern Recognition (CVPR)*, pages 12894–12904, June 2021.
- [Wang *et al.*, 2021] Wenhai Wang, Enze Xie, Xiang Li, Deng-Ping Fan, Kaitao Song, Ding Liang, Tong Lu, Ping Luo, and Ling Shao. Pyramid vision transformer: A versatile backbone for dense prediction without convolutions. In *Proceedings of the IEEE/CVF International Conference on Computer Vision (ICCV)*, pages 568–578, October 2021.
- [Woo *et al.*, 2018] Sanghyun Woo, Jongchan Park, Joon-Young Lee, and In So Kweon. Cbam: Convolutional block attention module. In *Proceedings of the European Conference on Computer Vision (ECCV)*, September 2018.
- [Xiao *et al.*, 2018] Tete Xiao, Yingcheng Liu, Bolei Zhou, Yuning Jiang, and Jian Sun. Unified perceptual parsing for scene understanding. In *Proceedings of the European Conference on Computer Vision (ECCV)*, September 2018.
- [Yang *et al.*, 2021] Jianwei Yang, Chunyuan Li, Pengchuan Zhang, Xiyang Dai, Bin Xiao, Lu Yuan, and Jianfeng Gao. Focal self-attention for local-global interactions in vision transformers. *CoRR*, abs/2107.00641, 2021.
- [Yates *et al.*, 2021] Andrew Yates, Rodrigo Nogueira, and Jimmy Lin. Pretrained transformers for text ranking: Bert and beyond. In *Proceedings of the 14th ACM International Conference on Web Search and Data Mining, WSDM ’21*, page 1154–1156, New York, NY, USA, 2021. Association for Computing Machinery.
- [Zhang *et al.*, 2022] Zizhao Zhang, Han Zhang, Long Zhao, Ting Chen, Sercan O Arik, and Tomas Pfister. Nested hierarchical transformer: Towards accurate, data-efficient and interpretable visual understanding. In *AAAI Conference on Artificial Intelligence (AAAI)*, volume 2022, 2022.
- [Zhao *et al.*, 2020] Hengshuang Zhao, Jiaya Jia, and Vladlen Koltun. Exploring self-attention for image recognition. In *Proceedings of the IEEE/CVF Conference on Computer Vision and Pattern Recognition (CVPR)*, June 2020.
- [Zhou *et al.*, 2017] Bolei Zhou, Hang Zhao, Xavier Puig, Sanja Fidler, Adela Barriuso, and Antonio Torralba. Scene parsing through ade20k dataset. In *Proceedings of the IEEE Conference on Computer Vision and Pattern Recognition (CVPR)*, July 2017.